

Thermal photon to dilepton ratio in high energy nuclear collisions

Jajati K. Nayak, Jane Alam, Sourav Sarkar, and Bikash Sinha

Variable Energy Cyclotron Centre, 1/AF, Bidhan Nagar, Kolkata 700064, India

(Received 8 July 2008; revised manuscript received 8 August 2008; published 4 September 2008)

The ratio of transverse momentum distribution of thermal photons to dilepton has been evaluated. It is observed that this ratio reaches a plateau beyond a certain value of transverse momentum. We argue that this ratio can be used to estimate the initial temperature of the system by selecting the transverse momentum and invariance mass windows judiciously. It is demonstrated that if the radial flow is large then the plateau disappears and hence a deviation from the plateau can be used as an indicator of large radial flow. The sensitivity of the results to various input parameters has been studied.

DOI: [10.1103/PhysRevC.78.034903](https://doi.org/10.1103/PhysRevC.78.034903)

PACS number(s): 25.75.Cj, 25.75.Dw, 24.85.+p

I. INTRODUCTION

Collisions between nuclei at ultrarelativistic energies produce charged particles—either in the hadronic or in the partonic state, depending on the collision energy. Interaction of these charged particles produce real and virtual photons (lepton pairs). Because of their nature of interaction, the mean free path of electromagnetic (EM) radiation is large compared to the size of the system formed after the collision. Therefore, EM radiation can be used as an efficient tool to understand the initial conditions of the system [1–5] and hence can be used to probe the quark gluon plasma (QGP) formation in heavy ion collisions (HIC). Practically, however, this is a difficult task, because on the one hand the thermal radiation from QGP has to be disentangled from those produced in initial hard collisions and from the decays of hadrons and on the other hand the evaluation of thermal photon and dilepton spectra need various inputs such as initial temperature (T_i), thermalization time (τ_i), equation of state (EOS), transition temperature (T_c), freeze-out temperature (T_f), etc., which are not known unambiguously. The sensitivity of the photon spectra to these inputs is demonstrated in Refs. [6] and [7]. Therefore, theoretical results on transverse momentum (p_T) spectra of photons and dileptons always suffer from these uncertainties. Of course, certain constraints can be imposed on these inputs from experimental results, e.g., transverse mass spectra of hadrons and hadronic multiplicities are useful quantities for constraining freeze-out conditions and initial entropy production.

In the present work, therefore, we evaluate the ratio of the transverse momentum spectra of thermal photons and lepton pairs,

$$R_{\text{em}} = (d^2 N_\gamma / d^2 p_T dy)_{y=0} / (d^2 N_{\gamma^*} / d^2 p_T dy)_{y=0}, \quad (1)$$

in which most of the uncertainties mentioned above are expected to get canceled so that it provides accurate information [8,9] about the state of the matter formed initially. We calculate the ratio R_{em} for SPS, RHIC, and LHC energies.

The article is organized as follows. In Sec. II we discuss the invariant yield of thermal photons and lepton pairs. In Sec. III, the space-time evolution is outlined. Results are presented in Sec. IV. Finally in Sec. V, we summarize the work.

II. PRODUCTION OF THERMAL PHOTONS AND e^+e^- PAIRS

The rate of thermal dilepton production per unit space-time volume per unit four-momentum volume is given by [1–3,5]

$$\frac{dN}{d^4 p d^4 x} = \frac{\alpha}{12\pi^4 M^2} L(M^2) \text{Im}\Pi_\mu^{\text{R}\mu} f_{\text{BE}}. \quad (2)$$

α is EM coupling, $\text{Im}\Pi_\mu^{\text{R}\mu}$ is the imaginary part of the retarded photon self energy, f_{BE} is the Bose-Einstein factor which is a function of $u^\mu p_\mu$ for a thermal system having four velocity u^μ at each space-time point of the system, $p^2 (= p_\mu p^\mu) = M^2$ is the invariant mass square of the lepton pair, and

$$L(M^2) = \left(1 + \frac{2m^2}{M^2}\right) \sqrt{1 - 4\frac{m^2}{M^2}} \quad (3)$$

arises from the final state leptonic current involving Dirac spinors. m in Eq.(3) is the lepton mass.

The real photon production rate can be obtained from the dilepton emission rate by replacing the product of the EM vertex $\gamma^* \rightarrow l^+l^-$, the term involving final state leptonic current, and the square of the (virtual) photon propagator by the polarization sum ($\sum_{\text{polarization}} \epsilon^\mu \epsilon^\nu = -g^{\mu\nu}$) for the real photon. Finally the phase space factor for the lepton pairs should be replaced by that of the photon to obtain the photon emission rate,

$$E \frac{dN}{d^4 x d^3 p} = \frac{g^{\mu\nu}}{(2\pi)^3} \text{Im}\Pi_{\mu\nu} f_{\text{BE}} \quad (4)$$

(see Refs. [1–3,5] for details).

The result given above is correct up to order $e^2 (\sim \alpha)$ in EM interaction but exact, in principle, to all orders in strong interaction. Now it is clear from Eqs. (2) and (4) that for the evaluation of photon and dilepton production rates one needs to evaluate the imaginary part of the photon self energy. The Cutkosky rules or thermal cutting rules give a systematic procedure to express the imaginary part of the photon self energy in terms of the physical amplitude.

A. Thermal photons

Ideally, one wants to detect photons from QGP. However, the experimental measurements contain photons from various processes, e.g., from the hard collisions of initial state partons

of the colliding nuclei, thermal photons from quark matter and hadronic matter, and photons from the hadronic decays after freeze-out. The contributions from the initial hard collisions of partons are under control via perturbative QCD (pQCD). The data from pp collisions will be very useful to validate pQCD calculations. Photons from the hadronic decays ($\pi^0 \rightarrow \gamma\gamma, \eta \rightarrow \gamma\gamma$, etc.) can be reconstructed, in principle, by invariant mass analysis. But the most challenging task is to separate the thermal photons originating from the hadronic phase, which needs careful theoretical estimation.

The invariant yield of thermal photons can be written as

$$\frac{d^2 N_\gamma}{d^2 p_T dy} = \sum_{i=Q,M,H} \int_i \left(\frac{d^2 R_\gamma}{d^2 p_T dy} \right)_i d^4 x, \quad (5)$$

where $i \equiv Q, M, H$ represents QGP, mixed (coexisting phase of QGP and hadrons), and hadronic phases, respectively. $(d^2 R/d^2 p_T dy)_i$ is the static rate of photon production from phase i , which is convoluted over the expansion dynamics through the integration over $d^4 x$.

1. Thermal photons from quark gluon plasma

The contribution from QGP to the spectrum of thermal photons due to annihilation ($q\bar{q} \rightarrow g\gamma$) and Compton ($q(\bar{q})g \rightarrow q(\bar{q})\gamma$) processes has been calculated in Refs. [10] and [11] using hard thermal loop (HTL) approximation [12]. Later, it was shown that photons from the processes [13] $gq \rightarrow gq\gamma, qq \rightarrow qq\gamma, qq\bar{q} \rightarrow q\gamma$, and $gq\bar{q} \rightarrow g\gamma$ contribute in the same order $O(\alpha_s)$ as Compton and annihilation processes. The complete calculation of emission rate from QGP to order α_s has been performed by resumming ladder diagrams in the effective theory [14]. In the present work this rate has been used. The temperature dependence of the strong coupling, α_s , has been taken from Ref. [15].

2. Thermal photons from hadrons

For the photon spectra from hadronic phase we consider an exhaustive set of hadronic reactions and the radiative decay of higher resonance states [16–18]. The relevant reactions and decays for photon production are (i) $\pi\pi \rightarrow \rho\gamma$, (ii) $\pi\rho \rightarrow \pi\gamma$ (with all possible mesons in the intermediate state [18]), (iii) $\pi\pi \rightarrow \eta\gamma$, and (iv) $\pi\eta \rightarrow \pi\gamma, \rho \rightarrow \pi\pi\gamma$, and $\omega \rightarrow \pi\gamma$. The corresponding vertices have been obtained from various phenomenological Lagrangians described in detail in Refs. [16–18]. The reactions involving strange mesons, $\pi K^* \rightarrow K\gamma, \pi K \rightarrow K^*\gamma, \rho K \rightarrow K\gamma$, and $K K^* \rightarrow \pi\gamma$ [19], have also been incorporated in the present work. Contributions from other decays, such as $K^*(892) \rightarrow K\gamma, \phi \rightarrow \eta\gamma, b_1(1235) \rightarrow \pi\gamma, a_2(1320) \rightarrow \pi\gamma$ and $K_1(1270) \rightarrow \pi\gamma$ have been found to be small [20] for $p_T > 1$ GeV. All the isospin combinations for the above reactions and decays have properly been taken into account. The effects of hadronic form factors [19] have also been incorporated in the present calculation.

B. Thermal dileptons

Like photons, dileptons can also be used as an efficient probe for QGP diagnostics, provided one can subtract out

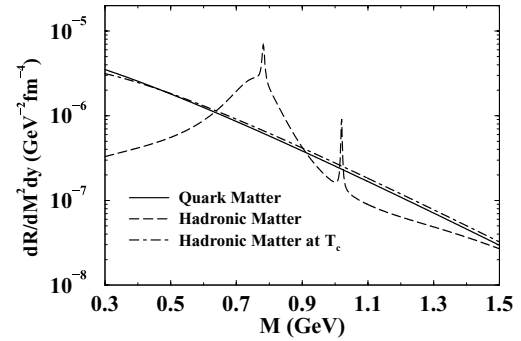


FIG. 1. The invariant mass distributions of thermal dileptons from QGP and hadronic matter at $T = 200$ MeV. Solid (dashed) line indicates the emission rates from QGP (hadronic matter). The dot-dashed line stands for emission rate from hadronic matter at the transition temperature (see text).

contributions from Drell-Yan processes, decays of vector mesons within the lifetime of the fire ball, and hadronic decays occurring after the freeze-out. Like hard photons, lepton pairs from Drell-Yan processes can be estimated by pQCD. The p_T spectra of thermal lepton pair suffer from the problem of indistinguishability between QGP and hadronic sources unlike the usual invariant mass (M) spectra that shows characteristic resonance peaks in the low M region. The invariant transverse momentum distribution of thermal dileptons (e^+e^- or virtual photons, γ^*) is given by

$$\frac{d^2 N_{\gamma^*}}{d^2 p_T dy} = \sum_{i=Q,M,H} \int_i \left(\frac{d^2 R_{\gamma^*}}{d^2 p_T dy dM^2} \right)_i dM^2 d^4 x. \quad (6)$$

The limits for integration over M can be fixed judiciously to detect contributions from either quark matter or hadronic matter (see Fig. 1). Experimental measurements [21,22] are available for different M windows.

1. Dileptons from QGP

In the plasma phase the lowest order process producing lepton pairs is $q\bar{q} \rightarrow \gamma^* \rightarrow l^+l^-$. QCD corrections to this rate have been obtained for a QCD plasma at finite temperature in Refs. [23] and [24] up to order $O(\alpha^2\alpha_s)$. In the present work contributions up to $O(\alpha^2\alpha_s)$ have been considered.

2. Dileptons from hadrons

The following parametrization [5,25] has been used to evaluate the dilepton emission rates from light vector mesons (ρ, ω , and ϕ):

$$\frac{d^2 R_{\gamma^*}}{dM^2 d^2 p_T dy} = \frac{\alpha^2}{2\pi^3} f_{\text{BE}} \left[\frac{f_V^2 M \Gamma_V}{(M^2 - m_V^2)^2 + (M \Gamma_V)^2} + \frac{1}{8\pi} \frac{1}{1 + \exp((w_0 - M)/\delta)} \left(1 + \frac{\alpha_s}{\pi} \right) \right]. \quad (7)$$

These parametrizations are consistent with the experimental data from $e^+e^- \rightarrow V(\rho, \omega \text{ or } \phi)$ processes [5,25,26]. Here, f_{BE} , is the Bose-Einstein distribution. f_V is the coupling between the EM current and vector meson fields, m_V and Γ_V are the masses and widths of the vector mesons, and ω_0 is the continuum threshold above which the asymptotic freedom is restored. We have taken $\alpha_s = 0.3$, $\delta = 0.2$ GeV, and $\omega_0 = 1.3$ GeV for ρ and ω . For ϕ we have taken $\omega_0 = 1.5$ GeV and $\delta = 1.5$ GeV. The EM current in terms of ρ , ω , and ϕ fields can be expressed as $J_\mu = J_\mu^\rho + J_\mu^\omega/3 - J_\mu^\phi/3$. Therefore, the contributions from ω and ϕ will be down by a factor of 9.

III. SPACE-TIME EVOLUTION

The matter formed after ultrarelativistic heavy ion collisions undergo space-time evolution, which can be described by relativistic hydrodynamics. In the present work the space-time evolution of the system has been studied using ideal relativistic hydrodynamics in (2+1) dimension [27] with longitudinal boost invariance [28] and cylindrical symmetry. The initial temperature (T_i) and thermalization time (τ_i) are constrained by the following equation [29] for an isentropic expansion:

$$T_i^3 \tau_i \approx \frac{2\pi^4}{45\xi(3)} \frac{1}{4a_{\text{eff}}} \frac{1}{\pi R_A^2} \frac{dN}{dy}, \quad (8)$$

where $dN/dy =$ hadron multiplicity, R_A is the radius of the system, $\xi(3)$ is the Riemann ζ function, $a = \pi^2 g/90$ ($g = 2 \times 8 + 7 \times 2 \times 2 \times 3 \times N_F/8$) is the degeneracy of the massless quarks and gluons in the QGP, and $N_F =$ number of flavors. The values of initial temperatures and thermalization times for various beam energies are shown in Table I. The initial energy density, $\epsilon(\tau_i, r)$, and radial velocity, $v_r(\tau_i, r)$, profiles are taken as

$$\epsilon(\tau_i, r) = \frac{\epsilon_0}{1 + e^{\frac{r-R_A}{\delta}}} \quad (9)$$

and

$$v_r(\tau_i, r) = v_0 \left(1 - \frac{1}{1 + e^{\frac{r-R_A}{\delta}}} \right), \quad (10)$$

where surface thickness $\delta = 0.5$ fm. We have taken $v_0 = 0$, which can reproduce the measured hadronic spectra at SPS and RHIC energies [6,30]. So far there is no consensus on the value of T_c ; it varies from 151 MeV [31] to 192 MeV [32]. In the present work we assume $T_c = 192$ MeV. In a first order phase transition scenario, we use the bag model EOS for the QGP phase and for the hadronic phase all the resonances with mass ≤ 2.5 GeV have been considered [33].

TABLE I. The values of various parameters—thermalization time (τ_i), initial temperature (T_i), freeze-out temperature (T_f), and hadronic multiplicity dN/dy —used in the present calculations.

Accelerator	$\frac{dN}{dy}$	τ_i (fm)	T_i (GeV)	T_f (MeV)
SPS	700	1	0.2	120
RHIC	1100	0.2	0.4	120
LHC	2100	0.08	0.7	120

To show the sensitivity of the results on the EOS we also use the lattice QCD EOS for $T \geq T_c$ [34]. For the hadronic matter (below T_c) all the resonances with mass ≤ 2.5 GeV have been considered [33]. For the transition region the following parametrization has been used [35].

$$s = f(T)s_q + (1 - f(T))s_h, \quad (11)$$

where s_q (s_h) is the entropy density of the quark (hadronic) phase at T_c and

$$f(T) = \frac{1}{2} \left(1 + \tanh \left(\frac{T - T_c}{\Gamma} \right) \right). \quad (12)$$

The value of the parameter Γ can be varied to make the transition strong or weak first order. Results for various values of Γ are given below.

IV. RESULTS

The values of the initial and freeze-out parameters shown in Table I along with the EOS mentioned above have been used as inputs to hydrodynamic calculations. The experimental data from SPS on hadrons [36], photons [37], and M distribution of dileptons [38] have been reproduced in Refs. [30], [39,40], and [41], respectively, by using these inputs. The values of the initial parameters for SPS agree with the results obtained from the analysis of photon spectra in Refs. [42–45]. Recently the data from the PHENIX Collaboration at RHIC [46,47] have also been explained in Ref. [6] (see also Ref. [48]) with the parameters mentioned in Table I. The lepton pairs measured by the NA60 Collaboration [49,50] in In-In collisions have been explained by spectral broadening of ρ [51,52].

The emission rate from hadronic and quark matter at a temperature of 200 MeV has been displayed in Fig. 1. The contribution from QGP dominates over its hadronic counterpart (without any medium effects) for $M < 600$ MeV and $M > 1.1$ GeV; therefore, these windows are better suited for the detection of QGP. However, it should be mentioned here that the modification of the spectral functions of vector mesons (especially ρ and ω)—pole shift [53] or broadening [26]—may give rise to dileptons at the lower M region making it difficult to detect contributions from QGP. The change in the hadronic spectral function will enhance the dileptons from the hadronic contribution in the lower mass ($M < 600$ MeV) window; however, the overall structure in the ratio R_{em} will not change appreciably. At the transition temperature (~ 200 MeV) if one assumes the vector meson masses go zero *a la* Brown-Rho scaling [53] then all the peaks in the dilepton spectra disappear and the rates obtained from EM current-current correlator (dot-dashed line) are close to the rate from QGP, indicating that the $q\bar{q}$ interaction in the vector channel has become very weak, signaling the onset of deconfinement. This also indicates the quark-hadron duality [54,55] near the transition point.

It is well known that the p_T spectra of photons and lepton pairs are sensitive to the values of initial temperature T_i , v_0 , T_f , and EOS. The T_c dependence of the p_T distribution is found to be negligibly small [6]. As we have mentioned before though these parameters can be constrained from the measured multiplicity and freeze-out spectra there remains

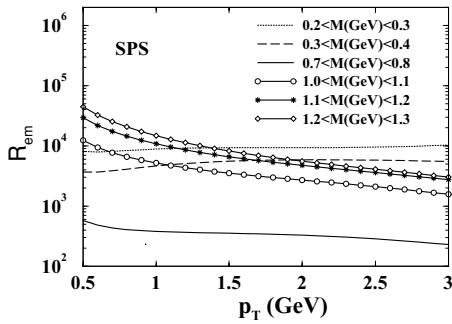


FIG. 2. The thermal photon to dilepton ratio, R_{em} , as a function of transverse momentum, p_T , for various invariant mass windows.

still some room to vary these quantities to be able to describe the experimental data.

The p_T dependence of the ratio R_{em} for SPS, RHIC, and LHC energies are shown in Figs. 2, 3, and 4, respectively. It is observed that at a given p_T , the ratio decreases with M , reaches a minimum around the ρ peak, and increases beyond the ρ peak. This trend is valid for all the cases, i.e., SPS, RHIC, and LHC, as expected because at a given p_T the R_{em} is actually the inverse of the invariant mass distribution of lepton pairs (the denominator, i.e., the photon spectra, is same for all the mass windows). It is observed from Figs. 2, 3, and 4 that the ratio R_{em} decreases with T_i for given p_T for M below the ρ peak and the opposite behavior is observed above the ρ peak. The slope of the ratio at low p_T also indicates substantial change with increasing M , the slope is minimum at the ρ peak. Therefore, the minimum of the slope may be used to locate the effective mass of the vector meson in medium.

It is clear from the results displayed in Figs. 2, 3, and 4 that the quantity, R_{em} , reaches a plateau beyond $p_T = 1.5$ GeV for all three cases, i.e., for SPS, RHIC, and LHC. It may be noted here that the degree of flatness increases from SPS to RHIC and LHC. As mentioned before for all three cases, except T_i all other quantities, e.g., T_c , v_0 , and EOS, are the same, so the difference in the value of R_{em} in the plateau region originates because of different values of initial temperature, indicating this can be a measure of T_i .

The following analysis is useful to understand the origin of the plateau at high p_T region. The strong three-momentum dependence in the dilepton and photon emission rates

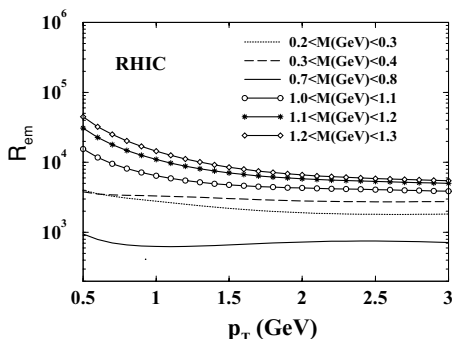


FIG. 3. Same as Fig. 1 for RHIC energy.

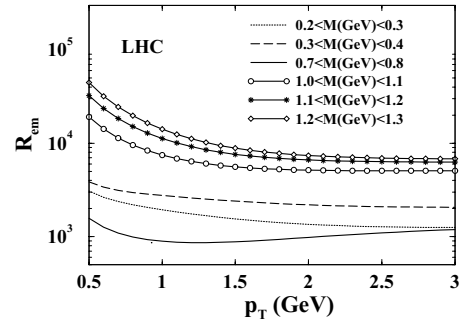


FIG. 4. Same as Fig. 1 for LHC energy.

[Eqs. (2) and (4), respectively] originates from the thermal factor, $f_{BE}(E, T)$. For a static system the energy, E , can be written as $E = M_T \cosh y$, where $M_T = \sqrt{p_T^2 + M^2}$, $y = \tanh^{-1} p_z/E$. At high $p_T (\gg M)$, $M_T \approx p_T$, the exponential momentum dependence becomes the same for real photon ($M^2 = 0$) and dilepton ($M^2 \neq 0$) spectra and hence a plateau is expected in the static ratio for large p_T for all the M values.

We recall that, for an expanding system out of the two kinematic variables describing the dilepton spectra, p_T is affected by expansion but M remains unchanged. The range of M under the present study is $0.3 < M \text{ (GeV)} < 1.3$. The energy, E , appearing in both the photon and dilepton emission rates should be replaced by $u^\mu p_\mu$ for a system expanding with space-time dependent four velocity u^μ . Under the assumption of cylindrical symmetry and longitudinal boost invariance, u^μ can be written as

$$u^\mu = \gamma_r(t/\tau, v_r \cos\phi, v_r \sin\phi, z/\tau), \quad (13)$$

where $\tau = \sqrt{t^2 - z^2}$, $t = \tau \cosh\eta$, $z = \tau \sinh\eta$, $v_r(\tau, r)$ is the radial velocity, and $\gamma_r(\tau, r) = (1 - v_r(\tau, r)^2)^{-1/2}$. The four-momentum $p^\mu = (M_T \cosh y, p_T, 0, M_T \sinh y)$, where $p_L = m_T \sinh y$. Therefore, for dilepton

$$u^\mu p_\mu = \gamma_r(M_T \cosh(y - \eta) - v_r p_T \cos\phi), \quad (14)$$

and for photon the factor $u^\mu p_\mu$ can be obtained by replacing M_T in Eq. (14) by p_T . The p_T dependence of the photon and dilepton spectra originating from an expanding system is predominantly determined by the thermal factor f_{BE} . Therefore, we discuss following three scenarios. (i) At high $p_T (\gg M)$, $M_T \approx p_T$, the exponential momentum

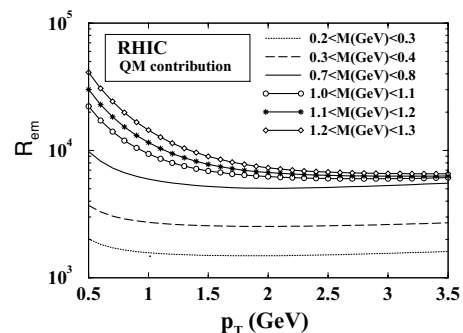


FIG. 5. Same as Fig. 2 for quark matter phase only.

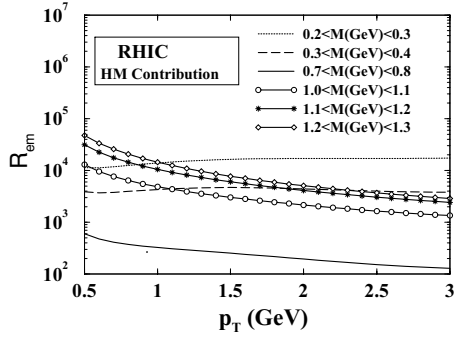


FIG. 6. Same as Fig. 2 for hadronic phase only.

dependence becomes the same for real photon and dilepton spectra; hence, for large p_T a plateau is obtained in the ratio R_{em} (Figs. 2–4). In other words, the effect of radial flow on the photon and dilepton is similar at high p_T regions. (ii) If the large M pairs originate from early (when the flow is small), the ratio R_{em} , which includes space-time dynamics, will be close to the static case and hence will show a plateau. (iii) However, at later times when the radial flow is large and M is comparable to or larger than p_T the effect of flow on the dilepton will be larger (receives larger radial kick due to nonzero M) than the photon and hence the plateau may disappear. Therefore, the disappearance of plateau structure in R_{em} in moderate or high M regions will indicate the presence of large radial flow. This can be understood from the results shown in Figs. 5 and 6.

In Fig. 5 the ratio has been displayed only for quark matter. Here the flow is expected to be lower within the present framework of the present study. A plateau is observed for all the M windows. It is observed that for high M (~ 1.2 GeV) and low M (~ 0.3 GeV) the ratio for QM is close to the total for LHC energy (not shown separately).

In Fig. 6 the ratios has been displayed for hadronic matter only. Here the flow is expected to be very large. Within the ambit of the present modeling the contribution from the hadronic matter is overwhelmingly large in the M region, $0.7 < M < 0.8$ GeV. Therefore, this region will have

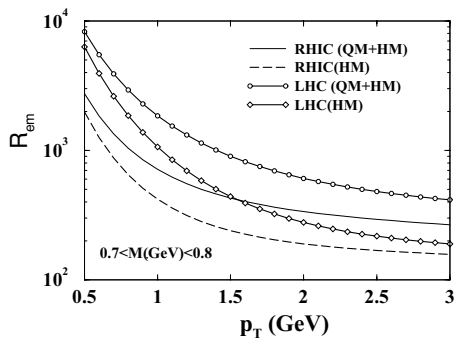


FIG. 7. The variation R_{em} with p_T for invariant mass window, $M = 0.7\text{--}0.8$ GeV. An unrealistically large value to radial flow has been given initially to demonstrate that large flow can destroy the plateau structure of R_{em} . Other inputs are similar to those of Figs. 3 and 4.

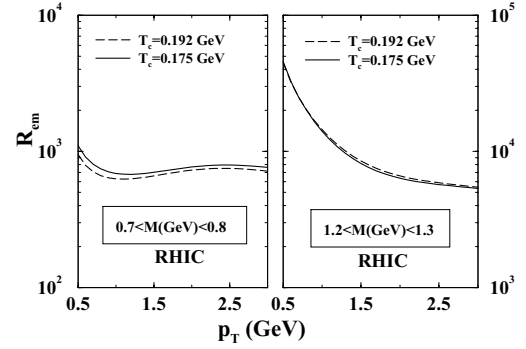


FIG. 8. R_{em} as a function of p_T for different values of T_c for invariant mass windows, $M = 0.7\text{--}0.8$ GeV and $M = 1.2\text{--}1.3$ GeV.

large effects from the radial flow and hence it may destroy the plateau. This is clearly seen in Fig. 6 for the curve corresponding to $0.7 < M < 0.8$ GeV.

To demonstrate the effect of flow on the plateau we use an initial velocity profile [which gives rise to radial flow stronger than that given by Eq. (10)] of the form $v_r(\tau_i, r) = v'_0 \frac{r}{R_A}$ with an *unrealistically* large value of $v'_0 \sim 0.5$. These inputs are used only for results shown in Fig. 7, which clearly indicates the disappearance of plateaus. Variation of R_{em} with p_T corresponding to the hadronic phase is steeper than the total because of larger radial flow in the late stage of the evolution.

Now we demonstrate the effect of other parameters on R_{em} . The value of T_c has large uncertainties. Therefore, we show the sensitivity of the results on T_c in Fig. 8 for two invariant mass windows. The results are insensitive to T_c .

The effect of the EOS on R_{em} is demonstrated in Fig. 9, by varying Γ in Eq. (12). It is observed that the effects of EOS on R_{em} for both the mass windows are small. Similar to the effect of T_c , the larger mass window ($1.2 \leq M$ (GeV) < 1.3) is less affected by the change in EOS. This is because the effects of radial flow (and other hydrodynamic effects) are less at early times from where higher mass lepton pairs originate. Replacement of lattice QCD EOS for the QGP phase by bag model shows negligible effects on R_{em} .

In Fig. 10 the dependence of R_{em} ($p_T = 2.5$ GeV) is depicted as a function of T_i for $1.2 \leq M$ (GeV) < 1.3 . This

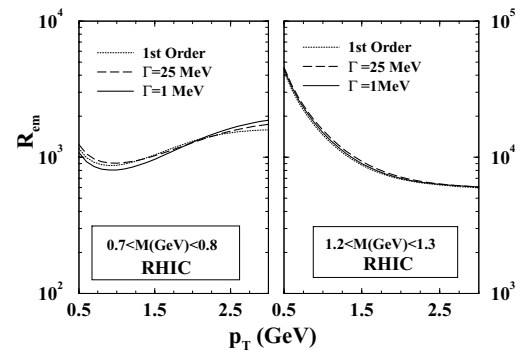


FIG. 9. R_{em} as a function of p_T for different EOS for invariant mass windows, $M = 0.7\text{--}0.8$ GeV and $M = 1.2\text{--}1.3$ GeV.

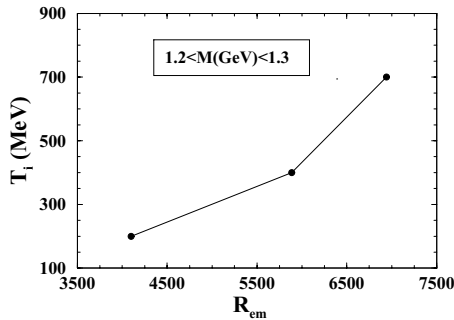


FIG. 10. Initial temperature is plotted as function R_{em} ($p_T = 2.5$ GeV) for the M window, $M = 1.2-1.3$ GeV.

mass window is selected because the contributions from the hot quark matter phase dominate this region and the effects of T_c , EOS, etc., are least here. $p_T = 2.5$ GeV is taken because R_{em} achieved a complete plateau at this value of transverse momentum. The change in R_{em} from SPS to RHIC is about 40% and from RHIC to LHC is about 20%. A simultaneous measurement of photons and dileptons with required accuracy will be useful to disentangle the effects of flow and true average temperature in a space-time evolving system formed in heavy ion collisions at ultrarelativistic energies.

We have evaluated R_{em}^{pQCD} , the ratio $(d^2N_\gamma/d^2p_T dy)_{y=0}/(d^2N_{\gamma^*}/d^2p_T dy)_{y=0}$, for hard processes using pQCD (Fig. 11). The hard photon contributions have been constrained to reproduce the PHENIX data [56] for pp collisions at $\sqrt{s_{NN}} = 200$ GeV. We consider $q\bar{q} \rightarrow \gamma^* \rightarrow l^+l^-$, $q\bar{q} \rightarrow g\gamma^*$, and $qg(\bar{q}) \rightarrow q\bar{q}\gamma^*$ for the lepton pair production. The M integration of lepton pair spectra [Eq. (6)] is carried out over the range $0.2 \leq M(\text{GeV}) \leq 0.3$. We observe that R_{em}^{pQCD} increases for p_T up to ~ 3 GeV, above which it reaches a plateau. Therefore, for $p_T \sim 1-3$ GeV, R_{em} for the thermal and pQCD processes show a different kind of behavior. The plateau arises from the fact that at large p_T both photons and dileptons show power law behavior [57,58]. In the low p_T domain lepton pairs (photon) from pQCD processes indicate a Gaussian type [57] (power law) variation resulting in the increase of R_{em} with p_T .

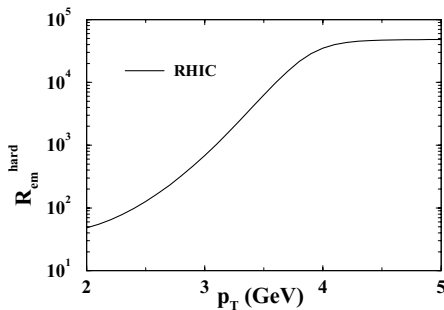


FIG. 11. The variation R_{em} for hard photons to dileptons ratio as a function of p_T for $\sqrt{s_{NN}} = 200$ GeV and invariant mass window, $M = 0.2-0.3$ GeV.

V. SUMMARY AND CONCLUSIONS

We have studied the variation of R_{em} , the ratio of the transverse momentum spectra of photons and dileptons, and argued that measurement of this quantity will be very useful in determining the value of the initial temperature of the system formed after heavy ion collisions. We have observed that R_{em} reaches a plateau beyond $p_T = 1.5$ GeV. The value of R_{em} in the plateau region depends on T_i . However, the effects of flow, EOS, and the dependence on the values of T_c , v_0 , and other model dependencies get canceled away in the ratio R_{em} . For M above and below the ρ peak and $p_T \geq 2$ GeV the contributions from quark matter dominates; therefore these regions could be chosen to estimate the initial temperature of the system formed after the collisions.

It is well known that T_{eff} , the inverse slope (see, e.g., Ref. [50]) extracted from the p_T spectra of EM radiation, contains the effect of temperature as well as flow. We have seen that when the flow is less (in the initial stage of the evolution) the ratio R_{em} shows a plateau for large $p_T (\gg M)$ and the height of the plateau in this region gives a good measure of the average temperature. However, a large flow can destroy the plateau and hence the deviation from the flatness of the R_{em} versus p_T curve may be used as a measure of flow. So a careful selection of M and p_T regions will be very helpful to disentangle the effect of the true average temperature and the flow (see also Ref. [59]). In Ref. [59] it was shown that the effects of flow on high $M (> 1.5$ GeV) could be quite large and in such cases the plateau in R_{em} may disappear. However, in the present work we confine in the range $0.3 < M(\text{GeV}) < 1.2$.

EM radiation originating from the interactions between thermal and nonthermal (high energy) partons [60–62] has been neglected in the present work. It is expected that the EM radiation from these processes and also from the pre-equilibrium stage will not affect R_{em} .

We have studied the effects of chemical off-equilibrium of mesons on the photon and dilepton production rates. This is implemented by appropriately introducing nonzero pionic chemical potential, μ_π ($\mu_\rho = 2\mu_\pi$, $\mu_\omega = 3\mu_\pi$), in the thermal factors [63] appearing both in photon and dilepton emission rates. We observed that the plateau structures in R_{em} do not change for RHIC and LHC, but for SPS they have little effect.

The change in hadronic spectral function at nonzero temperature and density is a field of high contemporary research interest as this is connected with the restoration of chiral symmetry in QCD. From the QGP diagnostics point of view the background contributions (photons and dileptons from thermalized hadrons) are affected because of medium effects on hadrons. Therefore, some comments on this issue are in order here.

We have checked that the p_T spectra of both photons and dileptons are sensitive to the pole shift of hadronic spectral function, as the reduction of hadronic masses [53] in a thermal bath increases their abundances and hence the rate of emission gets enhanced [5,16,17,39,40]. The invariant mass distribution of lepton pairs is sensitive to both the pole shift and broadening [26,40,41,64,65]. But the p_T spectra of the EM radiation is insensitive to the broadening of the spectral

function provided the integration over the M is performed over the entire region. This is because broadening does not change the density of vector mesons significantly (see also Ref. [40]). However, the number density of vector mesons depends on the nature (shape) of the spectral function within the integration limit. Therefore, the p_T spectra may change due to broadening when the integration over M is done in a limited M domain. We have checked that doubling the ρ width ($\sim 2 \times 150$ MeV) changes R_{em} by 10%. It is important to note that the change in mass and widths cannot be arbitrary;

it should obey certain constraints as discussed in Ref. [66]. Therefore, simultaneous measurements of p_T spectra and invariant mass distribution of real and virtual photons could be very useful in understanding the nature of medium effects on hadrons [40].

ACKNOWLEDGMENT

We are grateful to Ludmila Levkova for providing the lattice QCD results for the equation of state.

-
- [1] L. D. McLerran and T. Toimela, Phys. Rev. D **31**, 545 (1985).
 [2] C. Gale and J. I. Kapusta, Nucl. Phys. **B357**, 65 (1991).
 [3] H. A. Weldon, Phys. Rev. D **42**, 2384 (1990).
 [4] J. Alam, S. Raha, and B. Sinha, Phys. Rep. **273**, 243 (1996).
 [5] J. Alam, S. Sarkar, P. Roy, T. Hatsuda, and B. Sinha, Ann. Phys. **286**, 159 (2000).
 [6] J. Alam, J. K. Nayak, P. Roy, A. K. Dutt-Mazumder, and B. Sinha, J. Phys. G **34**, 871 (2007).
 [7] J. Alam, D. K. Srivastava, B. Sinha, and D. N. Basu, Phys. Rev. D **48**, 1117 (1993).
 [8] B. Sinha, Phys. Lett. **B128**, 91 (1983).
 [9] S. Raha and B. Sinha, Phys. Rev. Lett. **58**, 101 (1987).
 [10] J. Kapusta, P. Lichard, and D. Seibert, Phys. Rev. D **44**, 2774 (1991).
 [11] R. Bair, H. Nakkagawa, A. Niegawa, and K. Redlich, Z. Phys. C **53**, 433 (1992).
 [12] E. Braaten and R. D. Pisarski, Nucl. Phys. **B337**, 569 (1990); **339**, 310 (1990).
 [13] P. Aurenche, F. Gelis, H. Zaraket, and R. Kobes, Phys. Rev. D **58**, 085003 (1998).
 [14] P. Arnold, G. D. Moore, and L. G. Yaffe, J. High Energy Phys. **11** (2001), 057; P. Arnold, G. D. Moore, and L. G. Yaffe, J. High Energy Phys. **12** (2001), 009; P. Arnold, G. D. Moore, and L. G. Yaffe, J. High Energy Phys. **06** (2002), 030.
 [15] O. Kaczmarek and F. Zantow, Phys. Rev. D **71**, 114510 (2005).
 [16] S. Sarkar, J. Alam, P. Roy, A. K. Dutt-Mazumder, B. Dutta-Roy, and B. Sinha, Nucl. Phys. **A634**, 206 (1998).
 [17] P. Roy, S. Sarkar, J. Alam, and B. Sinha, Nucl. Phys. **A653**, 277 (1999).
 [18] J. Alam, P. Roy, and S. Sarkar, Phys. Rev. C **71**, 059802 (2005).
 [19] S. Turbide, R. Rapp, and C. Gale, Phys. Rev. C **69**, 014903 (2004).
 [20] K. L. Haglin, J. Phys. G **30**, L27 (2004).
 [21] S. Damjanovic (NA60 Collaboration), Nucl. Phys. **A783**, 327 (2007).
 [22] A. Toia, arXiv:nucl-ex/0805.0153.
 [23] T. Altherr and P. V. Ruuskanen, Nucl. Phys. **B380**, 377 (1992).
 [24] M. H. Thoma and C. T. Traxler, Phys. Rev. D **56**, 198 (1997).
 [25] E. V. Shuryak, Rev. Mod. Phys. **65**, 1 (1993).
 [26] R. Rapp and J. Wambach, Adv. Nucl. Phys. **25**, 1 (2000).
 [27] H. von Gersdorff, L. McLerran, M. Kataja, and P. V. Ruuskanen, Phys. Rev. D **34**, 794 (1986).
 [28] J. D. Bjorken, Phys. Rev. D **27**, 140 (1983).
 [29] R. C. Hwa and K. Kajantie, Phys. Rev. D **32**, 1109 (1985).
 [30] B. K. Patra, J. Alam, P. Roy, S. Sarkar, and B. Sinha, Nucl. Phys. **A709**, 440 (2002).
 [31] Y. Aoki, Z. Fodor, S. D. Katz, and K. K. Szab, Phys. Lett. **B643**, 46 (2006).
 [32] M. Cheng *et al.*, Phys. Rev. D **74**, 054507 (2006).
 [33] B. Mohanty and J. Alam, Phys. Rev. C **68**, 064903 (2003).
 [34] C. Bernard *et al.*, Phys. Rev. D **75**, 094505 (2007).
 [35] M. Asakawa and T. Hatsuda, Phys. Rev. D **55**, 4488 (1997).
 [36] H. Appelshauser *et al.* (NA49 Collaboration), Phys. Rev. Lett. **82**, 2471 (1999).
 [37] M. M. Aggarwal *et al.* (WA98 Collaboration), Phys. Rev. Lett. **85**, 3595 (2000).
 [38] G. Agakichiev (CERES Collaboration), Phys. Lett. **B422**, 405 (1998).
 [39] J. Alam, S. Sarkar, T. Hatsuda, T. K. Nayak, and B. Sinha, Phys. Rev. C **63**, 021901(R) (2001).
 [40] J. Alam, P. Roy, S. Sarkar, and B. Sinha, Phys. Rev. C **67**, 054901 (2003).
 [41] S. Sarkar, J. Alam, and T. Hatsuda, J. Phys. G **30**, 607 (2004).
 [42] F. D. Steffen and M. H. Thoma, Phys. Lett. **B510**, 98 (2001).
 [43] P. Huovinen, P. V. Ruuskanen, and S. S. Rasanen, Phys. Lett. **B535**, 109 (2002).
 [44] K. Gallmeister, B. Kampfer, and O. P. Pavlenko, Phys. Rev. C **62**, 057901 (2000).
 [45] D. Peressounko and Yu E. Pokrovsky, arXiv:hep-ph/0009025.
 [46] S. S. Adler *et al.* (PHENIX Collaboration), Phys. Rev. C **69**, 034909 (2004).
 [47] H. Buesching (PHENIX Collaboration), Nucl. Phys. **A774**, 103 (2006).
 [48] D. d'Enterria and D. Peressounko, Eur. Phys. J. C **46**, 451 (2006).
 [49] A. Araldi (NA60 Collaboration), Phys. Rev. Lett. **96**, 162302 (2006).
 [50] A. Araldi (NA60 Collaboration), Phys. Rev. Lett. **100**, 022302 (2008).
 [51] H. van Hees and R. Rapp, Phys. Rev. Lett. **97**, 102301 (2006).
 [52] J. Ruppert, C. Gale, T. Renk, P. Lichard, and J. I. Kapusta, Phys. Rev. Lett. **100**, 162301 (2008).
 [53] G. E. Brown and M. Rho, Phys. Rev. Lett. **66**, 2720 (1991).
 [54] E. V. Shuryak, Nucl. Phys. **A661**, 119 (1999).
 [55] R. Rapp, Nucl. Phys. **A661**, 33 (1999).
 [56] S. Adler (PHENIX Collaboration), Phys. Rev. D **71**, 071102 (2005).
 [57] R. K. Ellis, W. J. Stirling, and B. R. Webber, *QCD and Collider Physics* (Cambridge University Press, Cambridge, UK, 1996).
 [58] R. D. Field, *Application of Perturbative QCD* (Addison-Wesley, Reading, MA, 1989).
 [59] T. Renk and J. Ruppert, Phys. Rev. C **77**, 024907 (2008).

- [60] P. Roy, J. Alam, S. Sarkar, B. Sinha, and S. Raha, Nucl. Phys. **624**, 687 (1997).
- [61] R. J. Fries, B. Muller, and D. K. Srivastava, Phys. Rev. Lett. **90**, 132301 (2003).
- [62] L. Bhattacharya and P. Roy, arXiv:hep-ph/0806.4033.
- [63] H. van Hees and R. Rapp, Nucl. Phys. **A806**, 339 (2008).
- [64] G. Q. Li, C. M. Ko, and G. E. Brown, Nucl. Phys. **A606**, 568 (1996).
- [65] R. Rapp, G. Chanfray, and J. Wambach, Nucl. Phys. **A617**, 472 (1997).
- [66] S. Leupold, W. Peters, and U. Mosel, Nucl. Phys. **A628**, 311 (1998).